First-principles study of native defects in $CdGeAs_2$

Tula R. Paudel and Walter R. L. Lambrecht
Department of Physics, Case Western Reserve University, Cleveland, Ohio 44106, USA
(Received 6 May 2008; revised manuscript received 26 June 2008; published 28 August 2008)

First-principles results are presented for various native defects in $CdGeAs_2$ as function of the relevant elements' chemical potentials. The defect formation energies were calculated using fully relaxed 64 atom supercells by means of the full-potential linearized muffin-tin orbital implementation of the density-functional theory in the local-density approximation (LDA). The LDA band gap is adjusted using the LDA+U approach by introducing a semiempirical orbital dependent U shift to the s orbitals of Cd and Ge and the d orbitals of Cd. The transition energies of the vacancies V_{Cd}, V_{Ge}, and V_{As}, and antisites Ge_{Cd}, Cd_{Ge}, Ge_{As}, and As_{Ge} are calculated. Defect levels are interpreted in a simple-molecular orbital theory picture and the relation between Kohn-Sham band structures and transition levels is discussed. The vacancies are generally found to have higher energy of formation than the antisites. In particular, the somewhat deeper acceptor V_{Ge} is found to have the highest energy of formation among the defects studied. Among the three shallow acceptors (V_{Cd}, Cd_{Ge}, Ge_{As}), the lowest energy of formation is found for Cd_{Ge}, but only the Ge_{As} antisite is expected to be active in electron paramagnetic resonance (EPR). This is consistent with experimental data, establishing a link between the EPR-active center and the shallow acceptor responsible for optical absorption. Both Ge_{Cd} and As_{Ge} are found to be deep donors.

DOI: 10.1103/PhysRevB.78.085214 PACS number(s): 71.20.Nr, 71.55.Ht

I. INTRODUCTION

$CdGeAs_2$ is an important ternary chalcopyrite structure semiconductor, standing out because of its extremely high second-order nonlinear optical susceptibility ($\chi^{(2)}_{123}$ =472 pm/V) [1,2] combined with adequate birefringence for phase matching.[3] Because of its wide transparency window deep into the infrared (up to 12 μm wavelength), it has high potential for frequency conversion in the infrared region.[4] On the other hand it has relatively low band gap (~0.6 eV at room temperature)[5] and hence defect related optical absorption near the band gap may be a problem. One of the main impediments for further development of this material is the lack of knowledge on the native defect physics. Even with the recently developed horizontal gradient freeze technique,[6] the samples still have a large density of not well identified defects.

Experimentally, information about the defects has been gathered from a combination of optical absorption, photoluminescence, electron paramagnetic resonance (EPR), and transport measurements. The transport measurements[3,7] provide evidence for a shallow acceptor which is located at about 0.12 eV above the valence-band maximum (VBM). The samples are indeed usually p-type doped. The splitting of the valence band, in the presence of ionized acceptors (i.e., at room temperature) leads to a well characterized inter-valence-band optical transition at 0.22 eV or 5.5 μm. This feature is undesirable for frequency doubling of CO_2 laser lines. It can be suppressed by going to low temperature and thus avoiding the holes in the top valence band. However, even at low temperature optical absorption features are present, which were identified with a second deep acceptor.[8] Specifically, two absorption lines were found to be correlated and approximately split by the same valence band splitting as before, and hence this absorption was identified with transitions from the two valence bands to the deep acceptor. Turning to luminescence, two bands are observed, one associated with the shallow and the other with the deep acceptor. They basically correspond to donor-acceptor-pair recombination with a shallow donor, placed at 14 meV below the conduction band,[9] or perhaps merged with transitions from the conduction band minimum. From estimating the zero-phonon line and fitting the temperature dependence the deep acceptor was estimated to lie at 0.26 eV above the VBM.[8] Only one native defect EPR signal has been observed thus far in CdGe As_2.[10] It was found to be correlated with the shallow acceptor and to have a (not well resolved) fine splitting best simulated with two Cd and two Ge neighbors and thus identified with an acceptor on the As site. This suggested Ge_{As} as the shallow acceptor,[11] rather than the alternative acceptors $V_{Cd_{Ge}}$ but did not rule out other possibilities such as Si_{As} or C_{As}. The chemical nature of the deep acceptor or the shallow donor has not been identified.

Atomistic simulations for the native acceptor were reported by Pandey *et al.*[12] using empirical interatomic potentials. They provide information on defect energies of formation but not on electron energy levels because they are not quantum mechanical. They suggested antisites to have lower energy for formation than Frenkel and Schottky pairs. Coulombic effects are included to study the acceptor binding energy between a hole and the ionized acceptor. The validity of these classical rather than quantum mechanical calculations is questionable. The embedded quantum cluster model was used to study the antisite acceptor defects as well as Si and C on As site by Miguel *et al.*[13] They concluded that Ge on As site was shallower than the other IV_{As} impurities. In short, no previous first-principles quantum mechanical calculations of the defect levels and energies of formation have been performed. In this paper we present first-principles calculations of vacancies and antisites.

II. COMPUTATIONAL METHOD

We used the density-functional theory (DFT) along with the full-potential linearized muffin-tin orbital (FP-LMTO)[14] method in the local spin-density approximation (LSDA) in a supercell approach. In this version of the FP-LMTO method, the envelope functions are smoothed Hankel functions and the decay of the Hankel function and degree of smoothing are controlled by parameters κ and the smoothing radius. Both of these are optimized to minimize the total energy. Our basis set includes s,p and d orbitals. The smooth part of the charge density, wave functions and potentials are obtained on a mesh of 44 divisions in each direction in the primitive unit cell of bulk $CdGeAs_2$. The Brillouin zone (BZ) is sampled with a shifted $4\times4\times4$ regular mesh. For the defect supercells, the number of points is scaled accordingly, i.e., increased in real space and decreased in reciprocal space.

The band gap in $CdGeAs_2$ is so strongly underestimated by the LDA that the gap becomes negative. To overcome this problem, we use the LSDA+U approach[15] in its spherically averaged version.[16] This method is usually applied only to strongly localized narrow bands and reflects the stronger Coulomb interactions in such bands than described by the orbital independent LSDA. Here it is applied to the Cd$-d$ bands as well as to the Cd$-s$ and Ge$-s$ orbitals. The Cd $-d$ bands, being completely filled, are shifted down by the LSDA+U correction. U_d is essentially chosen so as to obtain the correct position of the Cd$-d$ bands as known from, e.g., photoemission. This in turn affects the VBM, which is mostly As$-p$ like, through the $p-d$ coupling. This, however, would not be sufficient to fully correct the gap.

Somewhat more unusual is our application of the LSDA $+U$ approach to the mostly empty Cd$-s$ and Ge$-s$ orbitals. The justification for this is somewhat different. The remaining gap underestimate is due to the quasiparticle self-energy, which is by no means a localized atomic effect. However, since the conduction band states near the bottom have primarily Cd$-s$ and Ge$-s$ character, the most important effect is obtained by only including matrix elements of the self-energy between these orbitals. Very schematically, in the static approximation $\Sigma=iGW$, with G as the Green's function and W as the screened Coulomb interaction, becomes essentially the screened Hartree-Fock approximation ρW, with ρ as the density matrix. The screened W is here treated simply as an adjustable parameter U. Taking into account the correction of double counting (for what is already in LDA), the orbital dependent potential shift in the "spherical" LSDA $+U$ approach becomes

$$V_m = U_m\left[\frac{1}{2} - \rho_m\right], \tag{1}$$

where m labels the orbital, the density matrix ρ_m is obviously diagonal for s orbitals and is just an occupation number. Thus for empty orbitals, the potential is shifted up by $U_m/2$. Similarly the filled d orbitals are shifted down. It should be noted that this is essentially a projection operator $\hat{V}=|\phi_m\rangle V_m\langle\phi_m|$, with ϕ_m the radial wave function at the LMTO linearization energy E_ν which is only nonzero within the muffin-tin sphere. We emphasize that U_s is not an internal atomic parameter and should thus not be transferable from one Cd or Ge containing compound to another. It is a specific correction for $CdGeAs_2$, mimicking what a GW calculation would produce. It can significantly affect defect total energies by changing the population of defect energy levels due to the opening of the gap. Without this correction, these defect levels would become resonances and control over how to populate them for different charge states would be lost. In reality the conduction band also has important components in the interstitial region and hence a somewhat large and empirically determined U_s needs to be applied to effectively shift up the corresponding diagonal terms of the LMTO Hamiltonian. Also, since the valence bands contain small contributions from these orbitals, they will be slightly affected as well. Still, we find that by a judicious choice of the U_m parameters, a band structure is obtained with only slightly changed valence bands, and a band gap in close agreement with experiment. The advantage is that this same Hamiltonian can now be applied to the defect problem and will hence have built in the correct shifts of the defect levels depending on their degree of conduction or valence-band character. A similar approach using Zn$-s$ orbital was recently used by us for ZnO in a study of the oxygen vacancy.[17]

To model the defects, we here use a supercell size of 64 atoms, which is a $2\times2\times1$ supercell of the face-centered tetragonal (fct) conventional cell of the chalcopyrite structure, containing 16 atoms. A similar cell size was used previously for $ZnGeP_2$ defect studies.[18,19] This size should be sufficient for qualitative conclusions on the nature of the defect states. The atomic positions for each defect are allowed to fully relax, which is facilitated by the capability of the FP-LMTO method to calculate forces. A conjugate gradient method is used to do the minimization. However, we keep the unit-cell volume fixed at that of the perfect bulk crystal because we are interested essentially in the dilute limit of the defect's behavior rather than in its behavior at the high concentration implied by the supercell size. Charged states are dealt with by adding a compensating homogeneous background charge density. The periodic array of charged defects in a background charge density has an electrostatic contribution to the total energy which should go to zero in the dilute limit but may converge rather slowly. According to Leslie and Gillan[20] and Makov and Payne[21] the dominant correction for this effect scales as $1/L$ with L the linear supercell size. This term arises from a set of point charges in a background density. However, this model, even when including also quadrupole terms, as done by Makov and Payne, assumes the validity of a multipole expansion and may overestimate the correction, in particular for the more delocalized defects.[22] We provide a simple estimate of the point-charge correction in the form[23]

$$\Delta E = \frac{9q^2}{5R\epsilon}, \tag{2}$$

where R is the radius corresponding to a sphere of the same volume as the supercell (in atomic units) $4\pi R^3/3=V_{sc}$, i.e., $R=13.67\ a_0$, ϵ is the static dielectric constant, for which the value 16.2 is used[24] and the energy is in rydberg. This cor-

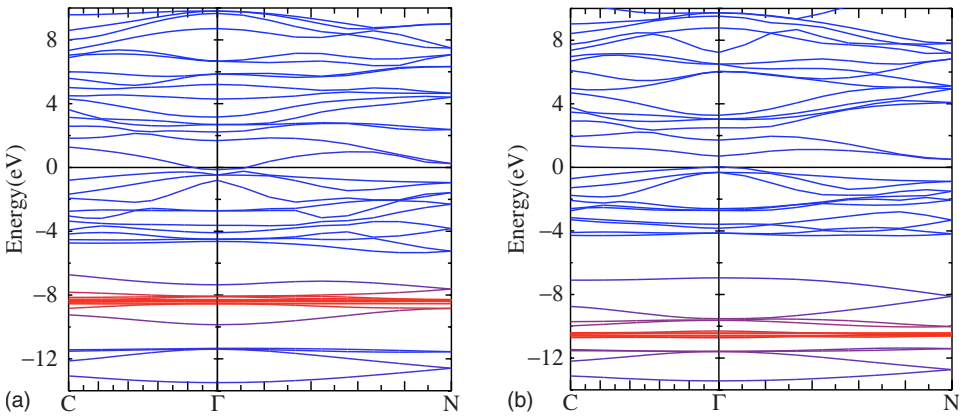

FIG. 1. (Color online) Energy bands (in eV) of $CdGeAs_2$ in LDA (left), LSDA+U_d+U_s (right). In the colored online version, the Cd−d bands are indicated in red and the hybridization of Cd−d with other bands is indicated by the continuous mixing of the red and blue color of the other bands to the degree of the Cd−d content. In the printed gray scale version this information is hard to see but described in the text.

rection amounts to 0.1106 eV for $q=1$. Including this correction tends to push up transition levels for acceptors and to push down transition levels for donors. Because this correction gives in some sense an upper limit of the shifts based on a pure point-charge model, we also give the results without the correction. In fact, for defect states for which we find a very delocalized character of the defect charge density, it is preferable not to use the Makov-Payne correction at all.

The energies of formation for different charge states q,

$$\Omega_f(D,q;E_F) = E_{sc}(D) - E_{sc} + \mu_{\text{removed}} - \mu_{\text{added}} + q(E_{vbm} + E_F), \tag{3}$$

and transition energies

$$\epsilon(q,q') = \frac{\Omega(D,q;0) - \Omega_f(D,q';0)}{q' - q} \tag{4}$$

are defined as usual. Here $E_{sc}(D)$ and E_{sc} are the supercell total energies (minus the energies of the free atoms) for the system with and without the defect, E_{vbm} is the bulk valence-band maximum energy with respect to the electrostatic potential reference energy in the supercell, and E_F is the Fermi level measured from the valence-band maximum. In this formalism, $\mu_{\text{removed/added}}$ are the chemical potentials of the added or removed elements. The latter are restricted to a certain range by considerations of thermodynamic equilibrium as will be further detailed in Sec. III.

A problem encountered in our present approach is that the LSDA+U total energies for $CdGeAs_2$ cannot be directly compared with the chemical potentials because the LSDA+U corrections applied are specific to the semiconductor compound $CdGeAs_2$ and do not apply for the reservoirs. The total energy changes are consistent with the potential shifts which affect the band structure and are not negligible. Thus, we have to be cautious in interpreting absolute energies of formation and focus mostly on transition energies, which are independent of the choice of chemical potentials. Differences in energy of formation between different defects will be addressed by calculations in LDA for the neutral state and adding the changes for different charge states as calculated within LSDA+U. The reason for choosing the neutral charge state is that this is the only one that makes physical sense for the metallic band structure obtained for $CdGeAs_2$ in LDA.

III. RESULTS

We present the results in several subsections. In Sec. III A, we present results on the band structure as function of the LSDA+U shifts. Next, we discuss the range of chemical potentials favorable to make $CdGeAs_2$. Next we present our results for the various defects and give a brief discussion of each case correlating the band structure with the transition levels. We classify the results in separate subsections on vacancies and antisites. Finally, we summarize the defect level positions and discuss the results in comparison with experimental data.

A. Band structure

It is well known that LDA underestimates band gaps in semiconductors. In this particular case it gives even a negative band gap at the center of the Brillouin zone. This would drastically change the nature of the defect states which would all become resonances in the bands. This means that one would occupy the wrong energy levels in studying charged defect states. Thus gap corrections are essential here. Underestimation of band gap in $CdGeAs_2$ arises in part because of the underestimate of the binding energy of the Cd d band. This was corrected by $U_d=2$ eV in Limpijumnong *et al.*[5] and gave a gap of 0.47 eV. However, in that paper, the atomic sphere approximation was used and a simple shift was added rather than a LSDA+U shift, in which the shift is at most $-U_d/2$ (if the occupation of the d orbital is 1) and the band is a pure Cd−d band. As discussed in Sec. II we further adjust the gap by adding U_s shifts to the Cd and Ge s orbitals. We use a value of $U_s=40.81$ eV for both Cd and Ge and $U_d=2$ eV on Cd to obtain a final gap of 0.67 eV, close to the low-temperature experimental gap.[8] These s-orbital shifts through the self-consistent rearrangements of the potential also cause the d band to further shift down. The final band structures are shown in Fig. 1. In this figure, the Cd−d orbital contribution to each band is indicated by the red color while the bands containing no Cd−d contribution are shown in blue. The colors are mixed to the degree of the hybridization. Since this information is only available in the online version, we clarify that the d bands occur just below −8 eV in the LDA in the middle of a band with strong Ge−s, As−p mixed character. In the LSDA+U_d+U_s picture, the d bands occur at −10.5 eV and the gap has significantly

opened. The conduction-band minimum actually occurs at the N-point. This is because the bands at this k-point have significant weight in the interstitial region and its shift is not properly accounted for by our shifts of only the Cd$-s$ and Ge$-s$ orbitals inside their respective muffin-tin spheres. In spite of this shortcoming, we have at least a gap comparable to the experimental gap and the valence bands are still very close to the LDA values. Thus we conclude that we have a satisfactory Hamiltonian to deal with the electronic states of $CdGeAs_2$ as well as its total energy and is therefore also suitable to address the defect states.

B. Chemical potentials

Determination of the range of the chemical potentials for the elements in $CdGeAs_2$ requires the knowledge of the cohesive energies of the bulk elemental solids Cd, Ge and As, and the energy of formation of several compounds that could potentially form: $CdAs_2$, Cd_2As_3, $GeAs_2$, GeAs, and of course $CdGeAs_2$. These compounds have different structures and their energy of formations have not all been determined. $CdAs_2$ is a tetragonal compound with D_4^{10} or $I4_122$ space group with four Cd atoms in the $4b$ positions and eight arsenic atoms in the $8f$ positions[25] with the energy of formation of the -0.182 eV/formula unit.[26] Cd_3As_2 is a tetragonal compound with space group $I4_1cd$ and its energy of formation was determined to be -0.43 eV/formula unit..[26] The compounds GeAs and the $GeAs_2$ are known to exist,[27,28] but their energy of formation has not yet been reported. GeAs is a tetragonal compound[29,30] and $GeAs_2$ has a complicated layered structure with space group P_{bam}.[28] We calculate the energy of formation of both these compounds to be positive, indicating that they are only metastable compounds. This means they do not provide a constraint on μ_{Ge}, which is then only limited by the formation of elemental Ge. For $CdGeAs_2$, we calculate an energy of formation of -0.61 eV in LDA. The excess chemical potentials, defined relative to the values in the bulk elements in their standard state at room temperature and ambient pressure, all must be negative to avoid precipitation of the elements.

The allowed range of excess chemical potentials is then determined by the following constraints:

$$\mu_{\mathrm{Cd}} + \mu_{\mathrm{Ge}} + 2\mu_{\mathrm{As}} = \Delta H_f(\mathrm{CdGeAs_2}),$$

$$\mu_{\mathrm{Cd}} + 2\mu_{\mathrm{As}} \leq \Delta H_f(\mathrm{CdAs_2}),$$

$$3\mu_{\mathrm{Cd}} + 2\mu_{\mathrm{As}} \leq \Delta H_f(\mathrm{Cd_3As_2}),$$

$$\mu_{\mathrm{Ge}} \leq 0. \tag{5}$$

These conditions determine the range of the chemical potentials for the formation of $CdGeAs_2$ as shown in Fig. 2. We may note that $CdGeAs_2$ allows for a rather wide range of chemical potentials and in particular allows a situation rich in Cd and Ge with both these chemical potentials being zero. This situation is rather different from $ZnGeP_2$.[18] The chemical potential of Zn in that case is strongly limited by the formation of Zn_3P_2 and hence a Zn-rich situation is not allowed and leads to a predominance of Zn vacancies. One

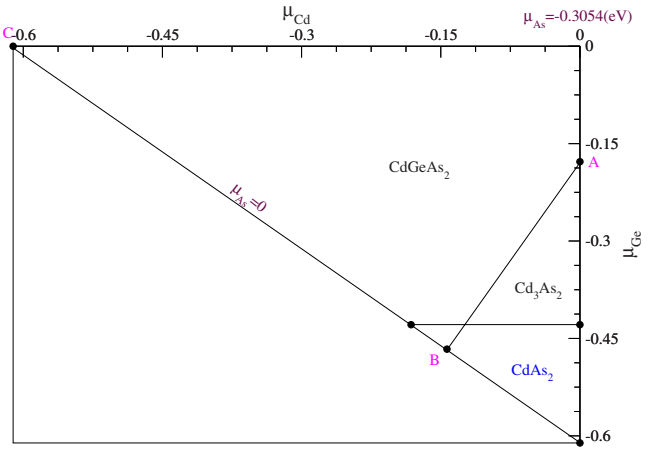

FIG. 2. (Color online) Chemical potential range in which $CdGeAs_2$ forms based on LDA calculations. The region of formation of $CdAs_2$ and Cd_3As_2 are indicated as well.

may already expect on the basis of the above diagram that the corresponding conclusion for Cd vacancies will not hold. Some points of particular interest for later are marked on the diagram. Point A corresponds to the lowest μ_{Ge} (Ge-poor) for the Cd-rich case. The point B is actually slightly out of the range of stability of $CdGeAs_2$; it corresponds to a Ge-poor, relatively Cd-rich but strongly As-rich situation ($\mu_{\mathrm{As}}=0$), in which case, it is already favorable to form Cd As_2. Case C corresponds to the Ge-rich, Cd-poor case.

C. Vacancies

1. Cadmium vacancy

The transition levels for the Cd vacancy are shown in Fig. 3 omitting the point-charge correction. The density of states (DOS) for various charge states are shown in Fig. 4. Removing a Cd atom leads to four As-like dangling bonds. In tetrahedral symmetry these form a deep a_1 level filled with two electrons and a t_2 level. The t_2 level will split into a b_2 and a doubly degenerate e level in the point group D_{2d} correspond-

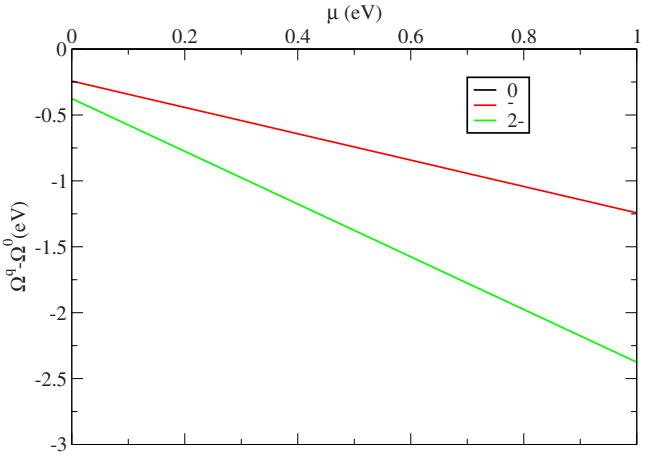

FIG. 3. (Color online) Differences in energy of formation of the cadmium vacancy (V_{Cd}) in various charge states. No transition levels occur, the defect being always in a double negative charge state.

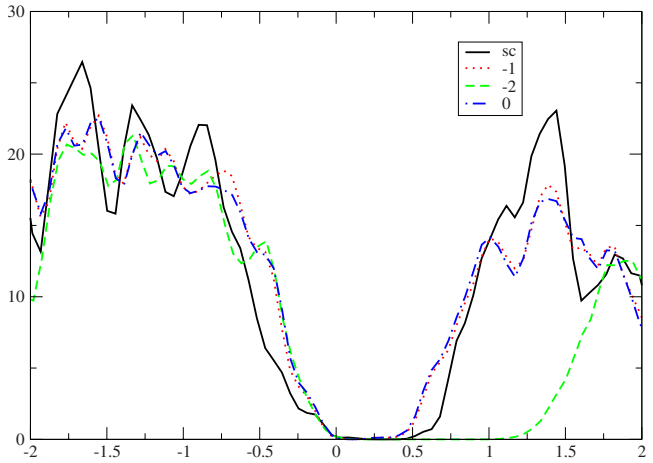

FIG. 4. (Color online) Density of states of the V_{Cd} defect in various charge states compared with the perfect crystal one.

ing to the tetragonal distortion of the chalcopyrite structure. Furthermore, however, the site symmetry (if we consider further than nearest neighbors) is lowered to S_4 in which case the e level splits further. The As dangling bonds point toward a Cd contain nominally each 1/2 and electron, so there are only two electrons to place in the e level (or its further split a and b levels) in the neutral state. Figure 4 shows that the DOS is enhanced compared to the perfect crystal in the energy range just below the VBM but no defect levels occur in the gap. This indeed indicates that the e level is present as a resonance below the VBM. In that case, the system should be in the 2− state for all values of the Fermi level above the valence-band maximum. It does not invalidate the charge neutrality because it is compensated by a positive uniform background charge density. This is indeed seen in Fig. 3. When adding the point-charge correction, the $2-/-$ level would move into the gap. However, because there are actually no single-particle levels in the gap, the defect charge density is very delocalized. In that case, it actually is preferable not to include the point-charge correction. In other words, the Cd vacancy defect potential, or at least its short-range part, is too weak to bind a defect level.

Now, in reality removing a Cd atom takes 2+nuclear (or core) charges away and hence there should be a long-range Coulomb tail in the defect potential. The latter cannot be captured by the relatively small supercell. Effective-mass theory would predict a shallow defect level to exist. It will be empty at low temperatures but could easily become singly or doubly ionized by emitting one or two mobile holes to the VBM. So, it is a double acceptor and may lead to the p-type behavior in $CdGeAs_2$ if this defect is present in abundance. We note that this level is shallower than for the Zn vacancy in $ZnGeP_2$.[18] This is mainly because the As levels have lower binding energy on an absolute scale (or relative to the Cd levels) than the P levels.

The relaxation of the surrounding As atoms around the Cd vacancy is inward by about 25 % and slightly larger for the 2− than the–and neutral charge states. Qualitatively, this agrees with the atomistic simulations by Pandey *et al.*[12] The distortion is mostly a breathing distortion with no clear evidence of any Jahn-Teller distortion within the precision of the relaxation calculations.

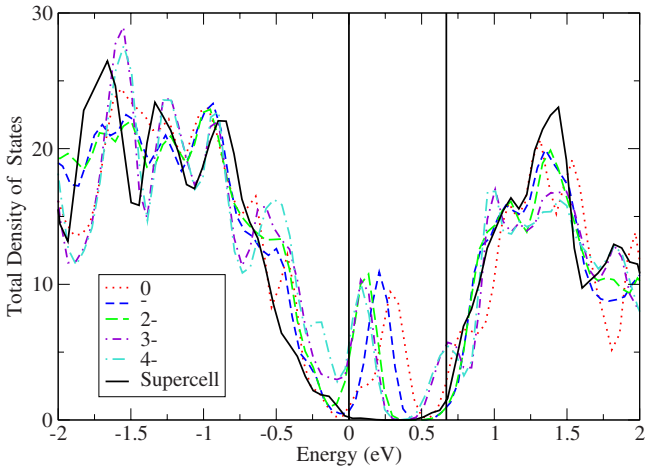

FIG. 5. (Color online) Density of states of the V_{Ge} for different charge states.

2. Germanium vacancy

The V_{Ge} is in principle a quadruple acceptor. The density of states (Fig. 5) clearly shows a defect band in the gap and shows it shifts for different charge states. We can also see an increase in density of states below the VBM.

The band structure (Fig. 6) for the neutral V_{Ge} shows two bands in the gap doubly degenerate at the Γ-point. This is the e level formed by the As dangling bonds, showing up as a peak in the gap in Fig. 5. It means that both the a_1 and b_2 level must be below the VBM and take the four electrons provided by the As dangling bonds in the neutral state. The e level can now take up to four extra electrons, leading to 1−, 2−, 3− and 4− charge states. The transition levels for the $0/-$ state thus clearly lie above the VBM. The $-/2-$ transition lies slightly higher. In this case, it is rather essential to take into account the point-charge correction, otherwise we obtain an erroneously low energy for the 3− and 4− charge states because of the scaling with q^2. This is also consistent with the more localized nature of this defect's charge density perturbation. Including the correction, we obtain Fig. 7.

3. Arsenic vacancy

On intuitive grounds, one might expect the V_{As} to be a donor. One expects levels to be formed from the Ge and Cd

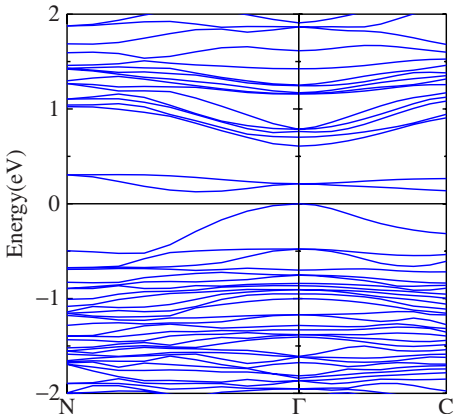

FIG. 6. (Color online) Band structure of the neutral V_{Ge} supercell.

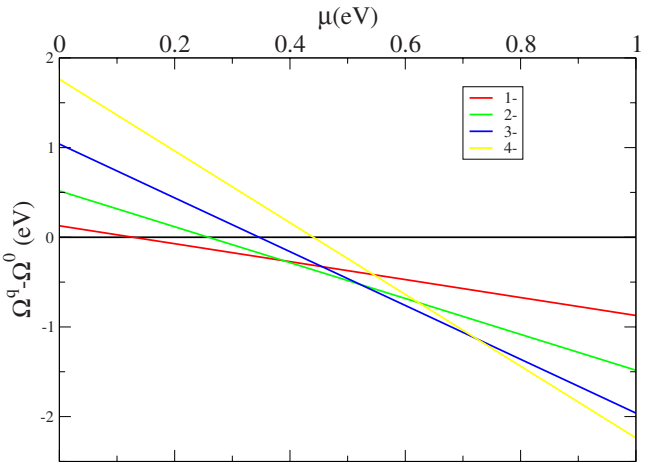

FIG. 7. (Color online) Differences in energy of formation of different charge states of the V_{Ge}.

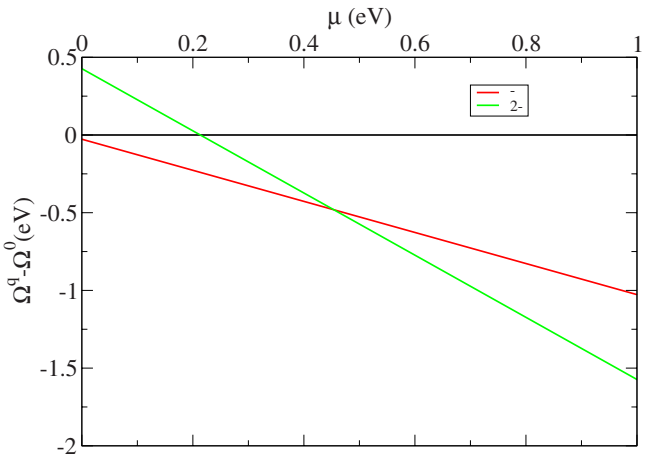

FIG. 9. (Color online) Differences in energy of formation for the V_{As}.

dangling bonds surrounding the vacancy. As in the case of the V_P case for $ZnGeP_2$ discussed by Jiang *et al.*[19] one expects the Ge dangling bonds to form the lower states. In that case, they form a deep level but still in the gap. Here, these levels are so low that they fall below the VBM. This means the two Ge-derived states must be fully occupied. Since the dangling bonds for the neutral state provide nominally only three electrons, it results in a single negative charge state as the ground state. The 2− charge state results from adding an electron in one of the Cd-derived dangling bonds.

The band structure (Fig. 8) shows indeed a defect band in the gap just below the conduction-band minimum as well as an extra band below the VBM. Note that the double degeneracy of some of the bands is lost because the site symmetry of the V_{As} site is C_2 only. Figure 9 shows the $-/2-$ transition at about 0.45 eV above the VBM. This corresponds to the results without Makov-Payne correction. This means that the defect would behave as an acceptor rather than a donor. When adding a Makov-Payne correction, this level moves above the conduction band but the $0/-$ level moves above

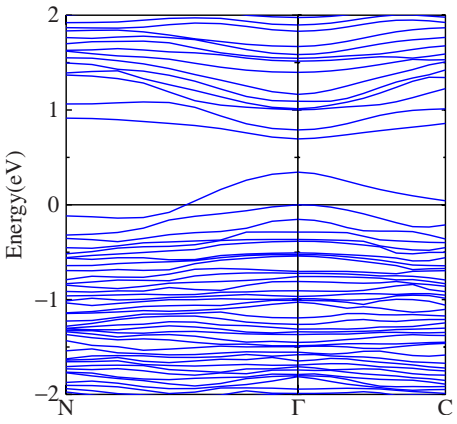

FIG. 8. (Color online) Band structure of the V_{As} in the neutral state. The band crossing the Fermi level (0 eV) is the VBM, the band just below it is Ge-dangling bond related band and the band split off just below the conduction band minimum is a Cd-dangling bond related band.

the VBM. However, since in the 1− state, the defect has no occupied one-electron level in the gap, the charge density is very delocalized and the Makov-Payne correction should not be included. On the other hand, adding an electron in the Cd-related dangling bonds does lead to a more localized charge density which should be corrected. In conclusion, this defect probably does not lead to any observable transition levels in the gap.

The Cd and Ge atoms surrounding the defect move inward toward the vacancy. In the case of the neutral defect, the Cd-Cd distance was reduced by 23% in comparison with the Ge-Ge distance which was reduced by 8%. The bond-length distribution around this defect is thus rather asymmetric. The local symmetry is no longer D_{2d} but only C_{2v} if we consider only nearest neighbors and only C_2 if we consider further neighbors. The mean Cd-As and Ge-As bond length decreased by 28% and 19%, respectively, with arsenic much closer to one of cadmium. The 1− charge state behaves similar to the neutral defect. But in the 2− state, the Cd-Cd distance is reduced by 22% while the Ge-Ge distance is reduced by 13%, in such a way that the Cd-As distance is reduced by 18% while the Ge-As distance is reduced by 23%.

D. Antisites

1. Cd_{Ge} *antisite*

The Cd_{Ge} antisite has many similarities with the V_{Cd}. Both are double acceptors. Again, no one-electron levels are found in the gap and the 2− charge state is found to have the lowest energy for all Fermi levels as seen in Figs. 10 and 11. This means again that the defect only introduces resonances below the VBM. Considering the long-range Coulomb effects, we conclude that a shallow acceptor level will exist. This defect shows very little relaxation compared with the vacancies discussed above. The inward relaxation of the surrounding As atoms is at most 1 %.

2. Ge_{Cd} *antisite*

The Ge_{Cd} antisite is expected to behave as a donor. A Ge on a Cd site imposes an attractive potential pulling down levels below the conduction band.

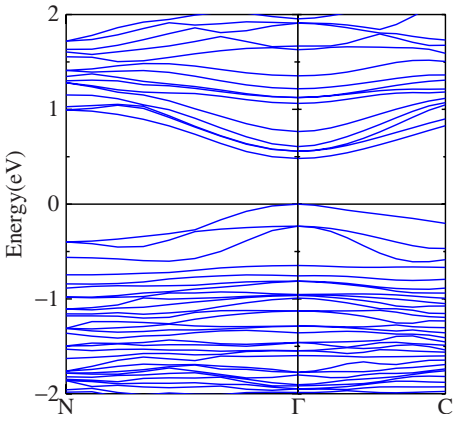

FIG. 10. (Color online) Band structure of the Cd_{Ge} antisite in the 2− state.

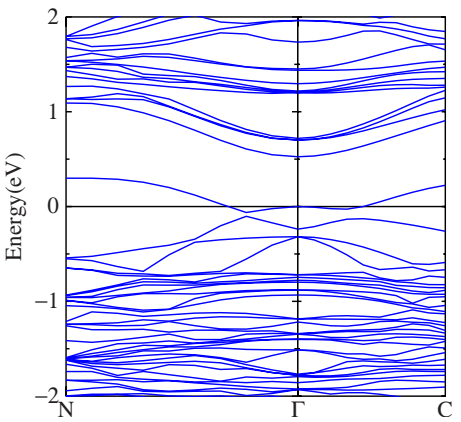

FIG. 12. (Color online) Band structure of the Ge_{Cd} antisite in the neutral charge state.

The band structure for the Ge_{Cd} antisite is shown in Fig. 12. It shows that one band is pulled so far below the conduction band that it actually crosses the VBM. The bands rehybridize and indicate anticrossing behavior at k-points along $\Gamma-N$ and $\Gamma-C$. The resulting separate band which has defect character away from Γ but VBM character near Γ can take either 0, 1, or 2 electrons, corresponding to the 2+, + and 0 charge states. Consistent with this picture, we find a $2+/+$ transition level right above the VBM and a $+/0$ transition level at about 0.22 eV above the VBM as can be seen in Fig. 13. When we add the Makov-Payne correction, the $+/0$ level moves down to about 0.11 eV, and the $2+/+$ transition level moves below the VBM. This means that the system cannot be in the 2+ charge state. As we mentioned above the "defect band" dips below the VBM at the center of the BZ. This means that band can never be completely emptied. So, instead of acting as a double donor as nominally expected, the Ge_{Cd} antisite effectively can only act as a single but still very deep donor. Adding the Makov-Payne corrections makes sense in this case because we do have a localized band in the gap. The reason for this very deep donor behavior is that Ge is not only to the right of Cd in the Periodic Table but also in an earlier row. So, it presents a very strongly attractive potential when placed on a Cd site. The relaxation of the atoms around the defect is again very small (less than 2%).

3. Ge_{As} *antisite*

The band structure (Fig. 14) for the Ge_{As} antisite shows no defect bands in the gap. Since Ge has one less electron than As, the neutral state would require one of the valence bands to be half filled. Since this is not possible in a semiconductor, it means that the lowest energy state of the defect is the single negative charge state. This is indeed seen in Fig. 15. It is in fact seen to be the lowest state for all Fermi level positions in the gap crossing the 2− level only at 0.62 eV. Although this is not a very localized level, and the Makov-Payne correction would probably be an overestimate, this crossing may be expected to rise even slightly higher. On the other hand, one might expect that the long-range Coulomb tail of the repulsive defect potential will lead to an effective mass like shallow acceptor state. In fact, according to the EPR studies, this is the most likely defect for the p-type doping, since its EPR signal (corresponding to the neutral state) is correlated with the inter-valence-band optical absorption resulting from the holes in the VBM and has hyperfine structure consistent with a group IV element surrounded

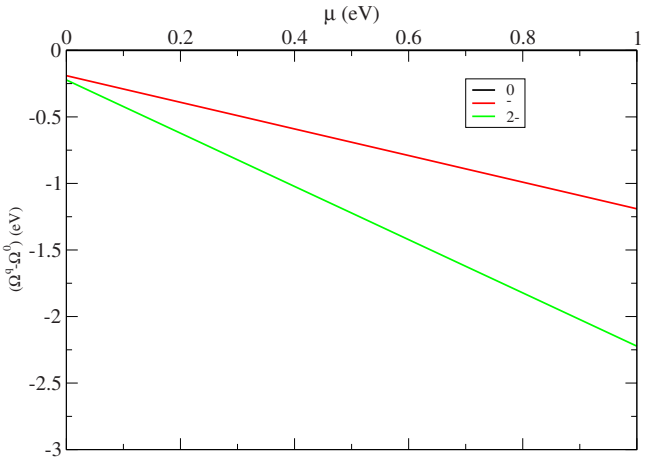

FIG. 11. (Color online) Differences in energy of formation for different charge states of the Cd_{Ge} antisite.

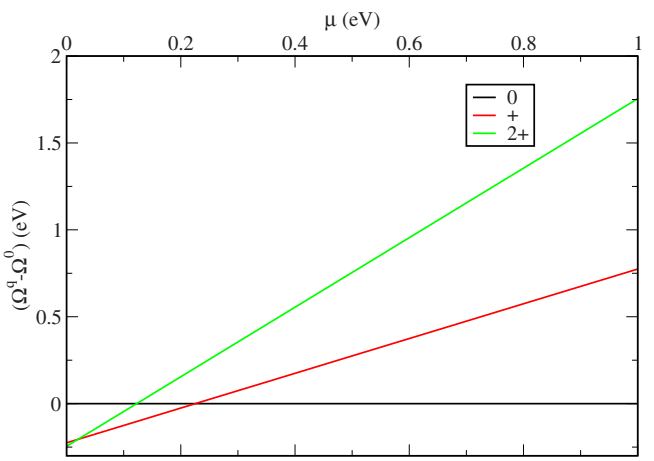

FIG. 13. (Color online) Differences in energy of formation of the Ge_{Cd} antisite.

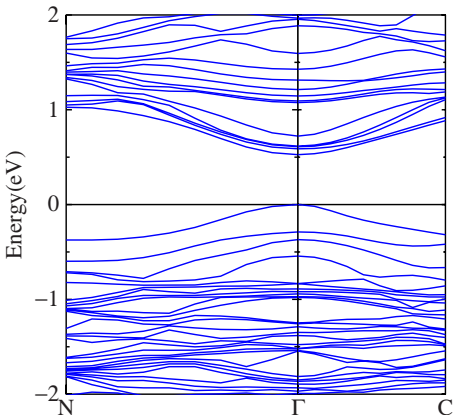

FIG. 14. (Color online) Band structure of the Ge_{As} antisite in the single negative charge state.

by two Cd and two Ge, i.e., on an As site. As for the other antisites, relaxations are small for this defect.

4. As_{Ge} *antisite*

The band structure for the As_{Ge} antisite (Fig. 16) shows a clear defect band in the gap which has conduction-band character. In fact, one expects again an attractive defect potential pulling levels down from the conduction band. This band would be half-filled in the neutral state because we added one extra electron. It is thus in principle amphoteric: It can either give the electron to the conduction band and act as a donor or it can accept a second electron and act as an acceptor.

In fact, we can see both a +0/ and 0/− transition level in Fig. 17 at 0.33 and 0.60 eV, respectively. This figure does not include the Makov-Payne corrections. Since the defect has a clearly defined defect level in the gap, we expect fairly localized charge density and hence adding the Makov-Payne correction makes sense. This pushes the donor level down to 0.22 eV and the acceptor level up to 0.72 eV above the conduction-band minimum. While the Makov-Payne correction may be an overestimate, it indicates that the defect has

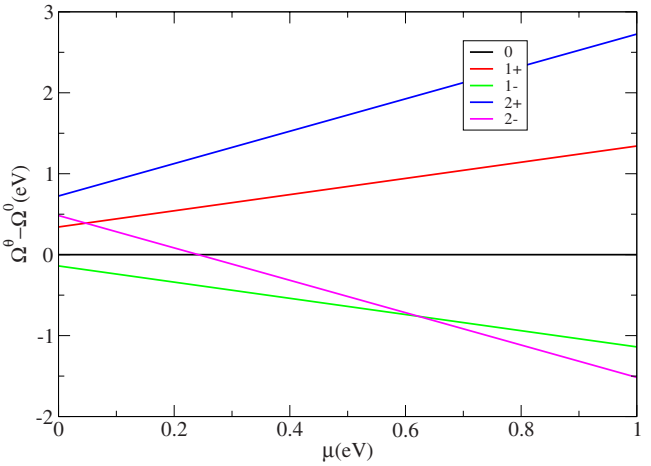

FIG. 15. (Color online) Differences in energy of formation for different charge states for the Ge_{As} antisite.

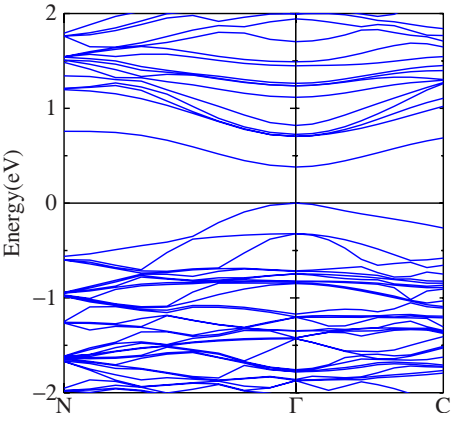

FIG. 16. (Color online) Band structure of the As_{Ge} antisite in the neutral charge state. The band in the gap is half filled, the zero of energy is the VBM.

more the character of a deep donor than that of an acceptor. The 1− state would not be accessible when pushed above the conduction-band minimum. The atoms relax slightly outward by at most 1.7 % for this defect.

E. Summary of defect levels

A summary of the expected defect transition levels in the gap is given in Table I and Fig. 18. The table gives all values without and with the point-charge correction. Negative values or positive values higher than the gap mean that strictly speaking this level is meaningless. As discussed in the previous sections, we selectively apply the point-charge Makov-Payne correction only to the cases with localized defect levels in the gap. In some cases, this removes certain states from the gap. We also indicate where we expect shallow defect levels based on the effective-mass theory but for which our small supercell does not give an actual defect level in the gap.

Next, we consider the absolute energies of formation of the defects to determine their relative abundances. As explained earlier, here we use LDA rather than LSDA+U for

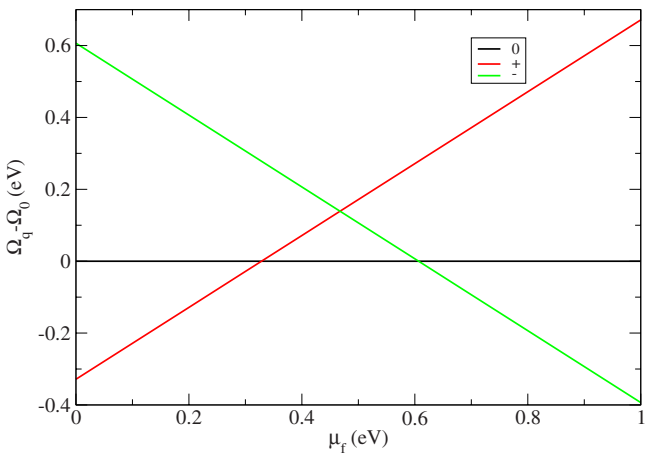

FIG. 17. (Color online) Differences in energy of formation for different charge states for the As_{Ge} antisite.

TABLE I. Transition levels (eV) of native defects in $CdGeAs_2$ without and with Makov-Payne point-charge correction.

Defect	q/q'	Without MP	With MP
V_{Cd}	0/−	−0.243	−0.132
	−/2−	−0.128	0.198
V_{Ge}	0/−	0.017	0.128
	−/2−	0.057	0.389
	2−/3−	−0.074	0.522
	3−/4−	−0.006	0.724
V_{As}	0/−	−0.022	0.089
	−/2−	0.454	0.786
Cd_{Ge}	0/−	−0.190	0.079
	−/2−	−0.030	0.300
Ge_{Cd}	2+/+	0.019	−0.313
	+/0	0.225	0.115
Ge_{As}	0/−	−0.139	−0.028
	−/2−	0.623	0.955
As_{Ge}	+/0	0.328	0.217
	0/−	0.606	0.717

TABLE II. Energy of formation (eV) of native point defects in the charge state of lowest energy when E_F=0, i.e., in *p*-type material, for different values of the chemical potentials as identified by points A, B, and C in Fig. 2 and given in the first three rows. The energy of formation for the neutral state of the defect is calculated in LDA and the difference from that state to the charge state under consideration is calculated in LSDA+U_d+U_s. The Makov-Payne correction was included for the cases indicated with a superscript * as discussed in the text.

Defect	Charge state	A	B	C
μ_{Cd}		0	−0.14	−0.61
μ_{Ge}		−0.18	−0.47	0
μ_{As}		−0.22	0	0
V_{Cd}	2−	1.53	1.39	0.92
V^*_{Ge}	0	3.67	3.38	3.85
V_{As}	1−	1.50	1.72	1.72
Ge^*_{Cd}	1+	1.51	1.66	0.72
Cd_{Ge}	2−	0.45	0.30	1.24
Ge_{As}	1−	0.82	1.32	0.86
As^*_{Ge}	1+	0.69	0.18	0.65

the neutral charge state and then add the difference for different charge states as calculated in LSDA+U_d+U_s. The neutral charge state is chosen here because in the metallic band structure obtained for $CdGeAs_2$ in LDA this is the only state that makes physical sense. Our emphasis of this section is on the energy differences between the different defects rather than on the absolute values themselves and we only wish to draw qualitative conclusions because of the inherent uncertainties in this procedure. The main open question is how well the LDA captures the energy of formation differences even in the neutral charge state. The results are shown in Table II. We choose to give the energy of formation of the defect in its charge state in *p*-type material, i.e., for the lowest energy charge state when the Fermi level is at the VBM. The Makov-Payne correction is only included in cases where strongly localized defect charges occur as discussed in the previous sections and is indicated by an asterisk. The chemical potential points A, B, and C correspond, respectively, to rich in both Ge and Cd, {Ge poor, As-rich}, and {Cd poor, Ge-rich}, respectively.

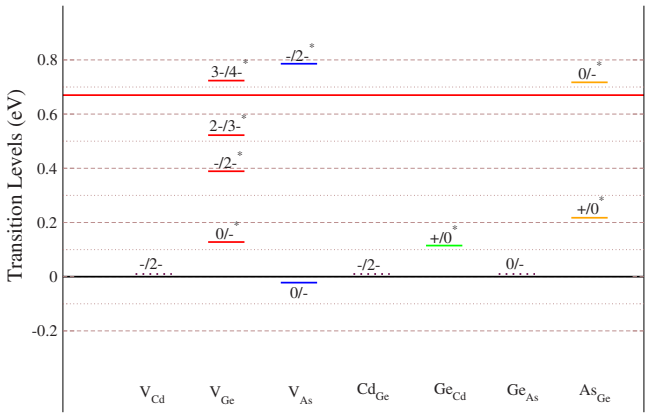

FIG. 18. (Color online) Summary of defect transition levels in the gap of $CdGeAs_2$. The levels for sufficiently localized defect states include the Makov-Payne point-charge correction, as indicated by ∗; the ones without ∗ do not include Makov-Payne correction. In cases where we expect a shallow level based on the long-range Coulomb tail and effective mass theory, we indicate the level by dotted lines.

We see from this table that the vacancies have generally higher energies of formation than the antisite defects. In particular, the V_{Ge} is the highest energy defect even in Ge-poor conditions. This was also the case in $ZnGeP_2$. In fact, we can see that the sum of the energies of formation of V_{Cd} and Cd_{Ge} is lower than the energy of formation of the V_{Ge}. This indicates that a V_{Ge} could lower its energy by having a nearby Cd being transferred to the Ge-vacancy site and creating a Cd-vacancy and then letting the two separate from each other by diffusion. This is true independent of chemical potential conditions. The Ge_{Cd} antisite has significantly higher energy than the Cd_{Ge} antisite. The lowest energy defect surprisingly is the As_{Ge} defect, for Ge-poor, As-rich situation B. Among the three candidate shallow acceptor defects, the lowest energy of formation is for the Cd_{Ge}, followed by the Ge_{As} antisite.

How does this compare with experimental results? The shallow acceptor responsible for the *p*-type doping has experimentally been correlated with the EPR spectrum assigned to the Ge_{As} antisite. We indeed predict this to be a shallow and relatively abundant acceptor. The calculations however predict that the Cd_{Ge} should be even more abundant. However, it is likely to be in the 2− state and therefore not EPR active, except at very low temperature.

The V_{Ge} which might have been considered to be a candidate for the deep acceptor based on its energy levels is unlikely to form as discussed above. This indicates that an impurity rather than a native defect might be responsible for

this deep acceptor. Also, the experimental energy level associated with a deep acceptor[8] is 0.26 eV, which does not match the values for the V_{Ge}. Thus we can safely rule out that the deep level is associated with the V_{Ge}. Among the native defects studied here, none is a shallow donor. Thus, the current models for luminescence that involve a shallow donor might instead involve direct transitions from the conduction band to the shallow and deep acceptor or an unknown impurity or defect complex must be invoked for the shallow donor. The absence of a native shallow donor, on the other hand, is compatible with the fact that $CdGeAs_2$ is unintentionally *p*-type.

The As_{Ge} antisite is predicted to be abundantly available in particular in As-rich Ge-poor material and would give an EPR signal in the neutral state, because then the defect band is singly occupied. This might require optical activation because in *p*-type material with the Fermi level near the VBM, this defect would be in the 1+ charge state. The Ge_{Cd} defect on the other hand would be EPR active in the 1+ state which is predicted to occur in *p*-type material as grown. However, this defect has a relatively high energy for formation and may thus not be present in the material in sufficient concentration to be detected.

IV. CONCLUSIONS

We have presented a comprehensive study of native defects in CdGe As_2. In order to overestimate the severe underestimate of the gap by LDA, we have used the LDA $+U_s+U_d$ approach, in which the Cd$-d$ levels are pushed down and both the Cd$-s$ and Ge$-s$ levels are pushed up, resulting in a realistic band structure with adjusted band gap. We find three candidate shallow acceptor defects among which the most abundant is predicted to be the Cd_{Ge} antisite, which however, is likely to be in the 2− charge state and hence not EPR active, except possibly at very low temperatures. We find Ge_{As} to be a relatively low formation energy antisite with shallow acceptor character. This is consistent with experimental observations. We find the V_{Ge} to be a high energy defect. If it can be formed, it would have relatively deeper acceptor character with three charge states (1−, 2−, 3−) in the gap. However, we find the V_{Ge} to be unstable toward the formation of a $V_{Cd}+Cd_{Ge}$ pair of defects. Its energy levels do not match the experimental position of the deeper acceptor. Two deep donors are identified Ge_{Cd} and As_{Ge}. Both however are very deep. The latter should be abundantly present in particular in As-rich, Ge-poor material and might be EPR activated by illumination, which could transfer an electron from the VBM to the +/0 level. Compared with $ZnGeP_2$, the acceptor levels are shallower and the donor levels of corresponding defects are deeper. This is because Ge is not only to the right of Cd but also in an earlier row. The relation between the Kohn-Sham band structures and the transition levels was discussed in detail for each defect. Since no native defects were identified which could correlate with the experimentally observed deep acceptor and shallow donors, we suggest that the latter may have their origin in impurities.

ACKNOWLEDGMENTS

This work was supported by the Air Force Office of Scientific Research under Grant No. F49620-03-1-0010. The calculations were done at the CWRU-HPC cluster and the Ohio Supercomputer Center.

[1] V. G. Dimitriev, G. G. Gurzadyan, and D. N. Nikogosyan, *Handbook of Nonlinear Optical Crystals* (Springer-Verlag, Berlin, 1991).
[2] S. N. Rashkeev, S. Limpijumnong, and W. R. L. Lambrecht, Phys. Rev. B **59**, 2737 (1999).
[3] D. W. Fischer, M. C. Ohmer, and J. E. McCrae, J. Appl. Phys. **81**, 3579 (1997).
[4] K. L. Vodopyanov and P. G. Schunemann, Opt. Lett. **23**, 1096 (1998).
[5] S. Limpijumnong and W. R. L. Lambrecht, Phys. Rev. B **65**, 165204 (2002).
[6] P. Schunemann and T. M. Pollak, J. Cryst. Growth **174**, 272 (1997).
[7] Y. V. Rud and V. Y. Rud, Jpn. J. Appl. Phys., Suppl. **32**, 672 (1993).
[8] L. Bai, N. C. Giles, and P. G. Schunemann, J. Appl. Phys. **97**, 023105 (2005).
[9] L. Bai, N. C. Giles, P. G. Schunemann, T. M. Pollak, K. Nagashio, and R. S. Feigelson, J. Appl. Phys. **95**, 4840 (2004).
[10] L. E. Halliburton, G. J. Edwards, P. G. Schunemann, and T. M. Pollak, J. Appl. Phys. **77**, 435 (1995).
[11] L. Bai, N. Y. Garces, N. Yang, P. G. Schunemann, S. D. Setzler, T. M. Pollak, L. Halliburton, and N. C. Giles, in *Progress in Semiconductors II-Electronic and Optoelectronic Applications*, MRS Symposia Proceedings No. 744, edited by B. Weaver, M. Manasreh, C. Jagadish, and S. Zollner (Materials Research Society, Pittsburgh, 2003), p. 537.
[12] R. Pandey, M. C. Ohmer, and J. D. Gale, J. Phys.: Condens. Matter **10**, 5525 (1998).
[13] M. A. Blanco, A. Costales, V. Luana, and R. Pandey, Appl. Phys. Lett. **85**, 4376 (2004).
[14] M. Methfessel, M. van Schilfgaarde, and R. A. Casali, in *Electronic Structure and Physical Properties of Solids. The Use of the LMTO Method*, Lecture Notes in Physics, edited by H. Dreyssé (Springer-Verlag, Berlin, 2000), Vol. 535, p. 114.
[15] A. I. Liechtenstein, V. I. Anisimov, and J. Zaanen, Phys. Rev. B **52**, R5467 (1995).
[16] S. L. Dudarev, G. A. Botton, S. Y. Savrasov, C. J. Humphreys, and A. P. Sutton, Phys. Rev. B **57**, 1505 (1998).
[17] T. R. Paudel and W. R. L. Lambrecht, Phys. Rev. B **77**, 205202 (2008).
[18] X. Jiang, M. S. Miao, and W. R. L. Lambrecht, Phys. Rev. B **71**, 205212 (2005).
[19] X. Jiang, M. S. Miao, and W. R. L. Lambrecht, Phys. Rev. B **73**, 193203 (2006).
[20] M. Leslie and M. J. Gillan, J. Phys. C **18**, 973 (1985).

[21] G. Makov and M. C. Payne, Phys. Rev. B **51**, 4014 (1995).
[22] D. Segev and S.-H. Wei, Phys. Rev. Lett. **91**, 126406 (2003).
[23] P. E. Blöchl, J. Chem. Phys. **103**, 7422 (1995).
[24] A. MacKinnon, *Physics of Ternary Compounds*, Landolt-Börnstein, New Series, Group III, Vol. 17, Pt. h (Springer, Berlin, 1985), pp. 97–99.
[25] L. Ĉervinka and A. Hrubý, Acta Crystallogr., Sect. B: Struct. Crystallogr. Cryst. Chem. **26**, 457 (1970).
[26] D. D. Wagman, *NBS Tables of Chemical Thermodynamic Properties* (National Bureau of Standards, Washington, D.C., 1982), Vol. 11.
[27] J. W. Rau and C. R. Kannewurf, Phys. Rev. B **3**, 2581 (1971).
[28] J. H. Bryden, Acta Crystallogr. **15**, 167 (1962).
[29] J. Osugi, R. Namikawa, and Y. Tanaka, J. Chem. Soc. Japan, Pure Chem. Sect. **87**, 1169 (1966).
[30] J. Osugi, R. Namikawa, and Y. Tanaka, Rev. Phys. Chem. Jpn. **37**, 81 (1967).